Supplementary Material for

Interdroplet bilayer arrays in millifluidic droplet traps from 3D printed moulds

Philip H. King, Gareth Jones, Hywel Morgan, Maurits R.R. de Planque and Klaus-Peter Zauner*

Electronics and Computer Science & Institute for Life Sciences, University of Southampton, Southampton, SO17 1BJ, United Kingdom.

*Corresponding author: kpz@ecs.soton.ac.uk

SUPPORTING MOVIES

Video keywords: millifluidic, microfluidic, interdroplet bilayer, droplet array, alpha-hemolysin, melittin, osmotic permeability, pillar trap, droplet rail

Video S1: Linear droplet array formation. This video demonstrates the creation of a 9-droplet alternating array in our millifluidic device. The droplets are 2 µL in volume, and contain red/green food dye 100-fold diluted in buffer solution. The video plays at 5× real time.

Video S2: Complex droplet array formation. This series of 5 runs demonstrates the formation of 1.5D droplet arrays. Three 0.7 µL droplets are sandwiched between a pair of 3 µL droplets, with the trailing buffer droplet being pushed into a central position forming a complex array. The stable formation of these arrays is achieved by the positioning of the 3 smaller droplets relative to the pillars that surround the capture area. The first pair of smaller droplets move sideways when disturbed by the arrival of subsequent droplets, blocking the gaps in between pillars in the capture area. The third (upper) droplet can then be moved into position between the initial pair by doubling or quadrupling the oil flow rate (initial flowrate 50 µL/min), before returning the oil flow to its initial rate once the complex array is formed. As seen in Run 5, this method is robust even if, as shown, the upper small droplet deviates away from the rail of the droplet trap. In Run 1, the droplets contain 500 mM KCl, 10 mM HEPES at pH 7.5, with the yellow droplets containing 250 µM fluorescein. In the subsequent runs, the droplets contain 1 M KCl, 10 mM HEPES at pH 7.0, with the blue droplets containing 250 µM erioglaucine disodium salt. The video plays at 3× real time.

Video S3: Osmotic water transport over bilayer. This video shows the osmotic transfer of water over interdroplet bilayers from a central low ionic strength droplet (4 µL, 0.25 M KCl, red) to a pair of flanking high-ionic strength droplets (2 µL, 1 M KCl, blue). The video plays at 40× real time.

Video S4: Action of melittin on interdroplet bilayers. A number of buffer-containing droplets are followed by a droplet containing 5 µg/mL melittin, a peptide which disrupts lipid bilayers via pore formation. The droplet containing melittin fuses repeatedly with the buffer droplets. The video plays at 15× real time.

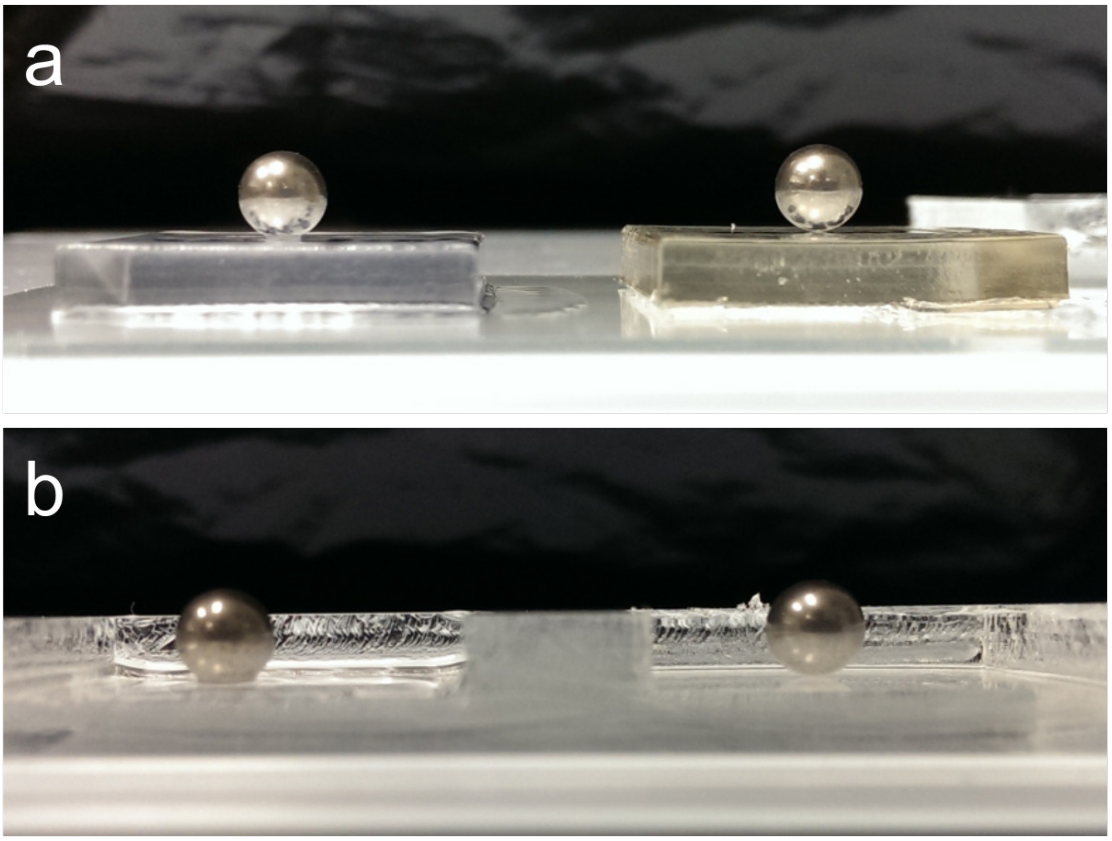

Figure and Video S5: Effect of baking 3DP moulds on the curing of PDMS. Untreated 3D-printed moulds were found to inhibit the curing of PDMS; baking the moulds eliminates the inhibitory effect. To demonstrate this, two 25 × 25 × 4 mm blocks of Objet VeroClear™ were printed on an Objet Connex350™ 3D printer. One block was baked for 24 hours at 80 °C, causing a colour change from grey to yellow. A degassed mix (10:1) of PDMS monomer and curing agent was poured over both blocks, and baked for 1 hour at 80 °C. At the interface between the untreated 3D printed block and the PDMS is an ≈ 0.5 mm deep zone in which the PDMS does not cure. A 4 mm diameter ball bearing placed on the untreated block after it is removed from the solidified PDMS sinks into the layer of uncured PDMS (*panel a, left*). No PDMS monomer is left behind on the surface of the baked block (*panel a, right*). The surface of the solidified PDMS that was in contact with the untreated block (*panel b, left*) is also covered with uncured PDMS. The PDMS surface in contact with the baked PDMS is clean (*panel b, right*). We have further visualised this effect in Video S5. A 4 mm diameter ball bearing was dropped onto each of the 3DP blocks. The bearing dropped onto the untreated block sinks into the uncured PDMS layer, whereas the bearing dropped on the treated block bounces and rolls away. The video plays in real time.

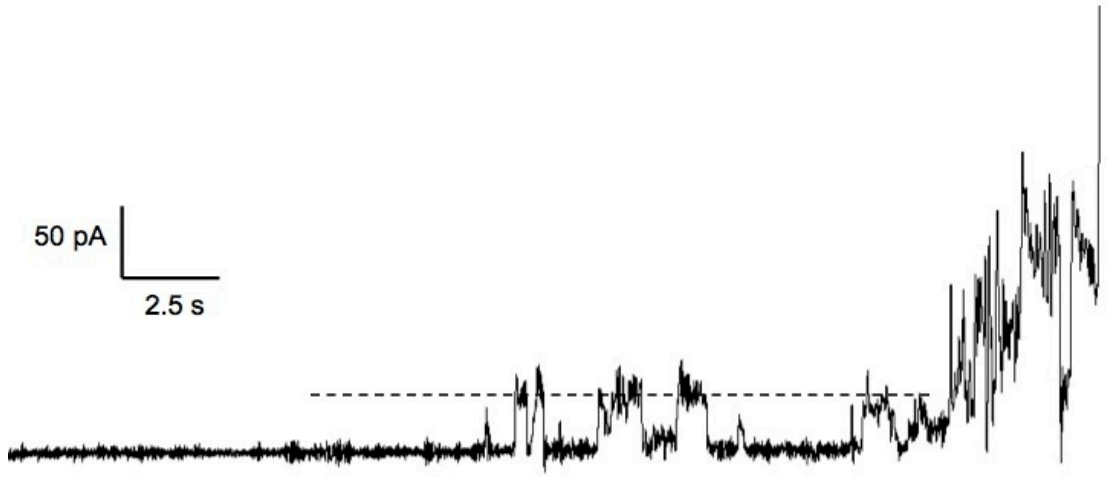

Figure S6: Single-channel current recordings in millifluidic droplet trap. Two droplets of 1 M KCl, 10 mM HEPES (pH 7.0) solution were trapped in the pillar array such that contact was made with the prepositioned Ag/AgCl electrodes. The interdroplet bilayer was voltage-clamped at +50 mV and the current signal was digitized at 5 kHz and a 20 Hz low-pass filter was applied. The bilayer was exposed to the water-soluble nanopore α-hemolysin, which was present in one of the droplets. The first of several discrete current steps, which are attributed to bilayer insertion of a single α-hemolysin channel, was observed approximately 45 s after interdroplet bilayer formation. The increase in bilayer current at the end of the recording, typical for rapid sequential insertion of multiple α-hemolysin nanopores, led to bilayer failure. The dashed line presents a 39 pA amplitude with respect to the baseline signal.

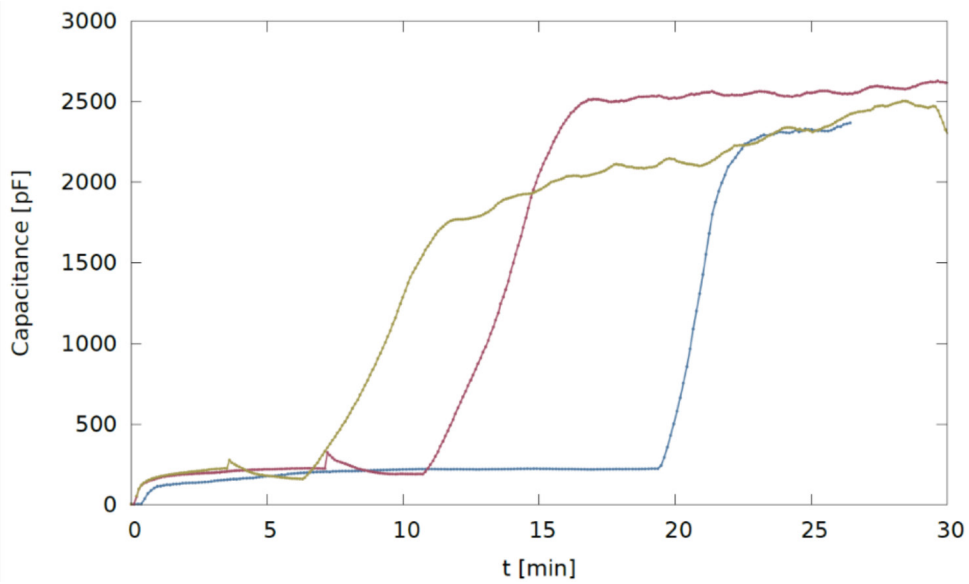

Figure S7: Capacitance measurements of interdroplet bilayers. Capacitance traces of interdroplet bilayers formed within the millifluidic device. The measurements were taken using a pair of Ag/AgCl electrodes, inserted into the chip in plastic pipette tips filled with agar through pre-punched holes in the roof of the droplet capture area. After the oil has been forced out of the bilayer, corresponding to the large increase in capacitance, the slow increase in capacitance observed could possibly be explained by the fact that one droplet becomes concave under the force of the constant oil flow, allowing a larger interface to form. The data presented here was captured in the same manner as that presented in Fig. 5 in the main paper.